Temperature Dependence of the Visible-Near-Infrared Absorption Spectrum of Liquid Water

Vaughan S. Langford, Allan J. McKinley, and Terence I. Quickenden*

Department of Chemistry, The University of Western Australia, 35 Stirling Highway, Crawley WA 6009, Australia

Received: January 7, 2001; In Final Form: May 30, 2001

Optical absorptivity spectra of ultrapure liquid water over the wavelength range from 550 to 900 nm and over the temperature range from ∼15 to 60 °C are presented. The measured temperature dependence compares well with those reported by most previous workers. The linear dependence of the absorption spectrum on temperature is discussed in terms of structural changes occurring in liquid water as a function of temperature. The two-state, outer-neighbor bonding model of Robinson and co-workers is found to provide a good microscopic explanation of our data.

Introduction

Water is ubiquitous on Earth and is essential for the existence of life. Among its many vital roles, it helps to moderate Earth's climate, especially because of the enormous reservoirs of liquid water in the oceans and of solid water in the polar regions. In addition, because its molecular vibrations are all infrared (IR) active, atmospheric water vapor is a very important greenhouse gas.

Because the radiation from the sun that reaches the Earth's surface comprises mainly near-UV, visible and near-infrared wavelengths, it is important that the optical properties of water in these regions, such as its absorptivity (a), should be characterized accurately for use in modeling studies. Moreover, because the absorptivity is temperature dependent, and water temperatures vary substantially across the planet, it is essential that temperature-dependent absorptivity coefficients of high accuracy are available. The benefits of such data are not only confined to the climate modeling community, but are also important to those needing reliable reference spectra as a function of temperature when they determine in situ spectra of natural waters.[1]

There have been several studies of the temperature dependence of the optical absorption of liquid water in the visible,[1−7] and near-IR[8−10] spectral regions. Studies in the near-IR region came first. Collins[8] published the temperature dependence from 0 to 95 °C of the absorption spectrum of liquid water in 1925. He obtained data from 700 to 2100 nm. Some years later, Waggener[9] and Luck[10] published work over similar spectral ranges, with Luck's work[10] covering a large range of temperatures (0 to 372.5 °C). Then Bell and Krohn[2] published a brief note describing the temperature dependence of two new visible absorption bands at 600 and 660 nm. Two decades later this work has been followed by a number measurements[1,3−7] that have sought to tabulate reliable absorptivity temperature coefficients (da/dT). It is clear from these measurements that at least in the range 2.5 to 40 °C, the absorption coefficient increases linearly with temperature. Hence in Figure 1 we summarize the earlier data by plotting the decadic absorptivity temperature coefficient as a function of wavelength. Note that the literature

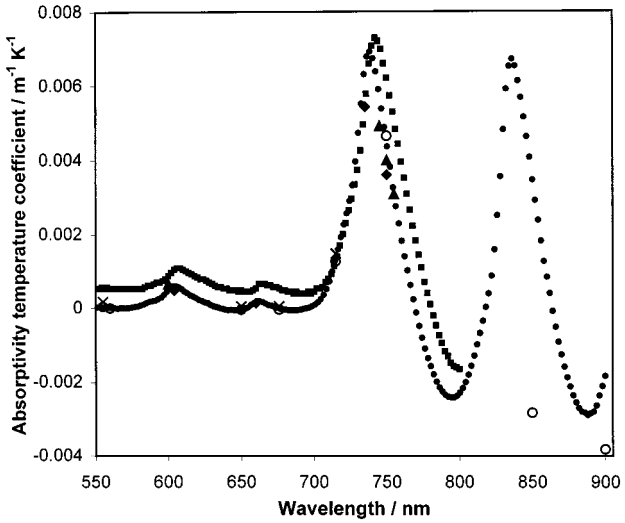

Figure 1. Decadic absorptivity temperature coefficients (da/dT) of liquid water obtained by Pegau and Zaneveld[4] (▲), Buiteveld et al.[5] (■), Pegau and Zaneveld[6] (×),Trabjerg and Højerslev[7] (♦), Pegau et al.[1] (○), and ourselves (•) are shown for the 550- to 900-nm wavelength range. The 95% confidence intervals for the data obtained here are smaller than the point sizes.

data[1,4−7] in Figure 1 were published as Napierian coefficients,[11] and were hence divided by $\log_e(10)$, before being replotted therein.

Højerslev and Trabjerg reported an average temperature-dependent absorption coefficient of 0.003 cm^{-1} K^{-1} from 400 to 600 nm over the temperature range 10−30 °C for a water sample with a 2-m path length.[3] However, the water purity was not specified. In later work,[7] they used water that had been double ion-exchanged and microfiltered in a cell with a 1-m path length. They measured the absorptivity of liquid water over the wavelength range 400 to 760 nm at temperatures from 6 to 30 °C. Their results[7] are shown in Figure 1 and are in reasonable agreement with those of other workers[1,4−6] for wavelengths longer than ca. 550 nm. However, at shorter wavelengths they find a small *decrease* in absorptivity with increased temperature, which is contrary to the results of other workers.[1,4−6] This

10.1021/jp010093m CCC: $20.00
Published on Web 09/08/2001

disagreement is possibly due to degradation of their water samples and/or changes in instrument response because each data set was acquired over a period of two to 3 weeks.

Pegau et al.[1,4,6] studied the optical absorption of water in the visible and near-IR regions over a total temperature range of ca. 5 to 33 °C (Figure 1). They used reverse osmosis to purify the water, and subsequently filtered it to remove particulates. Their earliest work[4] presented a continuous spectrum from 405 to 800 nm, which was obtained using a cell with a 0.10-m path length. Their next paper[6] used an absorption meter that sampled a total of only 12 wavelengths over the range 412 to 715 nm for samples with a 0.25-m path length. In their final paper,[1] they used several absorption meters with path lengths of 0.10 and 0.25 m, but increased the number of sampled wavelengths to 15, albeit over a wider wavelength range from 412 to 975 nm. They found[1] that the only statistically significant (≥ 0.0004 m^{-1} K^{-1}) temperature dependence in the visible region occurred at 610 nm; i.e., in the vicinity of the fourth overtone of the OH stretch.

Buiteveld et al.[5] have presented the most comprehensive tabulation of water absorption data as a function of wavelength and temperature, covering the range from 400 to 800 nm at 2 nm intervals and extending from 2.5 to 40.5 °C (Figure 1). These workers used a path length of 0.12 m and their water was purified by reverse osmosis followed by a single distillation step. Their absorptivity temperature coefficient is, however, somewhat larger than the results obtained by Pegau et al.[1,4,6]

A particular complication arises in such work because some of the temperature dependence studies have been made on natural waters, some of which were ocean waters containing high salt concentrations. In such cases, it is not expected that the temperature dependences will be comparable with those of highly purified water. In some cases, where purified water was examined, often to provide a reference point for natural waters, the amount of purification has been minimal and probably quite unsatisfactory. The early work of Højerslev and Trabjerg[3] is in this category.

In later work by these two authors[7] and in work by other authors,[1,5] studies on pure water were unfortunately carried out without full oxidative purification[12−15] of the water. This is essential in order to remove traces of organic impurities that may absorb light more strongly than the water itself and produce temperature dependences attributable to the organic impurity chromophore rather than to the water chromophore. The quality of the water samples used in such studies on even pure water is suspect because only ion-exchange, reverse osmosis and microfiltering were usually carried out, although in some cases a distillation step was also used. However, in no case was there an indication that oxidative distillation was part of the purification process. This procedure is necessary[12,15] if light absorbing organic impurities are to be removed. In such work, it is quite likely that the temperature dependence being measured is at least partly conditioned by the temperature dependence of an organic impurity chromophore, rather than by the water itself.

Furthermore, the utmost care must be taken to thoroughly clean the optical cells used in the absorption spectroscopic studies of weakly absorbing substances such as water.[12−15] Unfortunately, none of the temperature dependence studies discussed above make any mention of the procedures used for sample cell cleaning and preparation.

In the present work, we reinvestigated the temperature dependence of the absorptivity of liquid water using samples that are well-known to be ultrapure,[12,15] great care also being taken to carefully clean the surfaces of the optical cells and other components in contact with the water. Our aim was to provide definitive temperature dependence coefficients in the visible and near-IR regions, because there is considerable variability among the existing measurements in these regions (Figure 1). These results should be of considerable value to researchers in a wide range of fields. We attempt to interpret the observed temperature dependencies using existing structural models for liquid water.

Experimental Section

Spectroscopic and other Apparatus. The absorptivity of pure water in 10 cm silica cells was measured from 400 to 900 nm by using a GBC−UV 918 absorption spectrophotometer. The spectral slit width and step size were 2 nm.

The silica optical cells (Spectrosil) were placed in specially constructed thermostating brass cell blocks through which water from a temperature-regulated bath (Tronac PTC-40 temperature controller) could pass to produce the desired temperature. The temperature of the water in the cells was measured in situ by using a calibrated, glass-bead-encased thermistor as a resistance component in a Wheatstone bridge circuit and measuring the off-balance emf. The sample temperatures were usually stabilized to better than ±0.1 °C, except for measurements at around 60 °C, which were ±0.2 °C. Temperature stabilization of the water within the cells took about 40 to 50 min after a change in temperature.

The experimental data were obtained as follows. The absorptivity of liquid water from about 15 to 60 °C, with steps of ∼5 °C, was measured in double-beam mode vs an air reference. The data were subject to small, slow instrument drift as the temperature of the sample compartment changed with the cell block temperature. The effect of drift was eliminated as described in the Results section. Effects introduced by using an air reference were eliminated by subtraction of the reference spectrum for a given series of measurements (obtained at ca. 25 °C) from the data at all other temperatures.

The temperature range used was restricted to 15 to 60 °C for several reasons. First, a nitrogen purge to prevent condensation at temperatures lower than 15 °C tended to cause a large increase in drift during the scan and also increased spectral noise. Second, the upper limit was determined by a desire to avoid the release of bubbles from the heated water in the cells as these interfere with the passage of the light beam, and the ability of the thermostat bath to go to higher temperatures.

Water Purity. The water used in these experiments was purified by triple distillation according to the procedure described in detail previously.[12] Briefly, deionized water is distilled once using a commercial still, before two distillation steps in a custom-built, rigorously cleaned, borosilicate glass still. The first of these steps involves distillation under oxygen from an alkaline potassium permanganate solution in order to oxidatively remove organic impurities. The second step is a standard pure−water distillation. Both steps involve high splash-heads to prevent droplets of liquid being carried over in the steam. Water purified in this manner has a surface tension within experimental error of that accepted for ultrapure water and has a low level of particulates.[12] Absorption spectra of liquid water published by Quickenden and Irvin[12] and, more recently, by Litjens et al.[15] present absorptivities of the highly purified water from 196 to 320 nm and from 300 to 700 nm, respectively. Absorptivities in the UV[12,15] and red[15] regions are lower than those in earlier publications, which further demonstrates the high water purity (<1 ppb of UV-absorbing impurities).

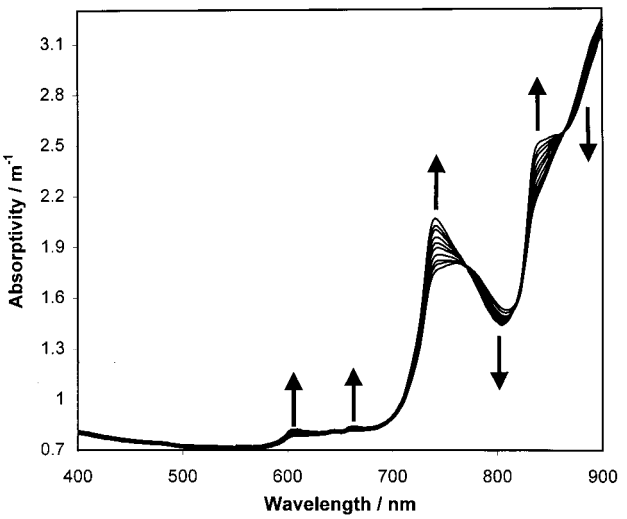

Figure 2. Typical raw absorptivity spectra of liquid water from 400 to 900 nm, over a temperature range of ~15 to 60 °C with temperature increments of ~5 °C. The sample path length was 10 cm, and the reference beam passed through air. The arrows indicate the direction of change of the absorptivity with increasing temperature. These data are from one of the eight runs that were averaged to give the data in Figure 1.

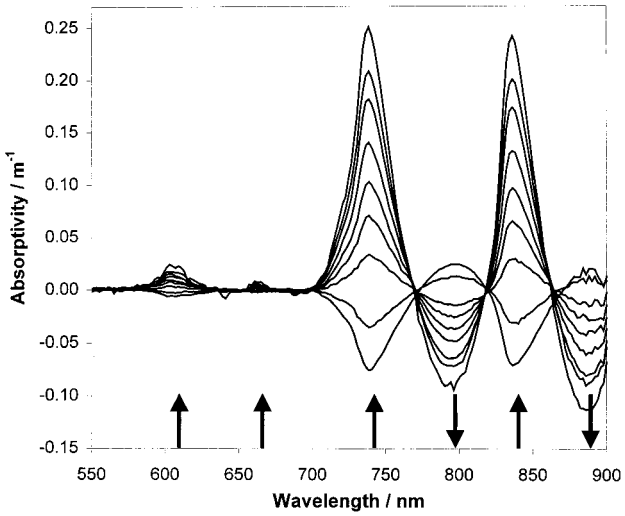

Figure 3. Typical differential absorptivity spectra for liquid water from 550 to 900 nm obtained by subtracting the 25.2-°C spectrum in Figure 2 from the spectra obtained at other temperatures from ~15 to 60 °C and correcting for instrument drift, as described in the text. The arrows indicate the direction of change of the absorptivity with increasing temperature.

For all but one run the water used was freshly distilled the preceding day, whereas for that run it was 3 days old. The same results were obtained.

Optical Cell Preparation. Besides using water of the highest purity, it is critical that all components contacting the water are carefully cleaned to remove compounds that would otherwise contaminate it. The optical cells, thermistors and cell caps were cleaned by the following procedure. First, they were cleaned for 2 h in a warm (~65 °C) 5% solution of Merck Extran MA01 alkaline cleaner in singly distilled water to remove organic impurities from the surface. Second, they were rinsed thoroughly with triply distilled water. Third, they were boiled in triply distilled water for ~30 min. Finally, they were rinsed thoroughly with triply distilled water. Thus, cleaned, the components were stored on lint free tissue away from dust. At all times the cells, thermistor and stopper were handled with dust-free latex gloves. Cell surfaces that would contact the triply distilled water never contacted the gloves.

Each day, before filling the cells with the water sample, the cells were rinsed three or four times with triply distilled water. The thermistor, and the stopper into which it was mounted, were also rinsed thoroughly.

Results

Figure 2 shows a typical series of absorptivity spectra obtained as a function of temperature. The absorptivity (linear decadic absorption coefficient; a) is derived from Beer's law

$$I = I_o \times 10^{-\epsilon c l}$$

Here, I_o and I are the incident and transmitted intensities, respectively, ϵ is the molar decadic absorption coefficient of the sample, c is its concentration, and l is the path length. For pure substances, such as liquid water, the absorptivity $a = \epsilon c$ is used, which has units of m^{-1}.

Figure 3 shows difference absorptivity spectra that were obtained by subtracting the spectra in Figure 2 from the 25.2 °C spectrum. The difference spectra often required further correction to account for instrumental drift due to the temperature changes in the sample compartment as the cell block was warmed or cooled. The procedure used was as follows. It was assumed that the absorptivity temperature coefficient in the 400- to 500-nm region was very small because the absorptivity is very low there.[13−15] The temperature dependence only takes on significant values near the overtone transitions of the OH stretch and their combination transitions with the bending vibrations (see Discussion), which are very weak in the blue.[13,14] Hence, a linear, sloping line was subtracted that best fitted the 400- to 500-nm region *and* the points at ~772, 816, and 864 nm where the absorptivity temperature coefficient is zero. Hence only the temperature coefficients in the 550- to 900-nm range are published, where the error introduced through neglect of temperature dependence in the lower 400- to 500-nm region will be less than the error bars on our spectra. Likewise, the temperature dependence of the scattering coefficient of liquid water was not considered because it was shown previously to be very small.[5,7]

Previous and present work shows that the absorptivity of liquid water has a linear dependence on temperature,[1,4−7] so the linear least-squares method was used to fit a straight line to the data of Figure 3 at each wavelength from 550 to 900 nm. Figure 4 illustrates the linearity for the data shown in Figure 3 at the peak maxima at 604, 660, 738, 796, 836, and 888 nm. Figure 5 summarizes the data at all wavelengths by giving the best-fit slope. It gives the results not only for the data illustrated in Figures 2 and 3, but also for the seven other runs that were performed using air as the reference. Four of these series of data were obtained with increasing temperature and four with decreasing temperature in an attempt to determine any faults in the data that produced hysteresis. None was observed, which adds to the credibility of the data. There is no observable difference between these runs within the experimental uncertainty, which is shown only for the run illustrated in Figures 2 and 3 for reasons of clarity. The uncertainty in each case is the 95% confidence interval in the absorptivity temperature coefficient calculated from the standard error in the slope of data like that in Figure 4.

Figure 1 and Table 1 show the mean absorptivity temperature coefficient and Table 1 gives its 95% confidence interval, which is always smaller than the point size used in Figure 1. The figure

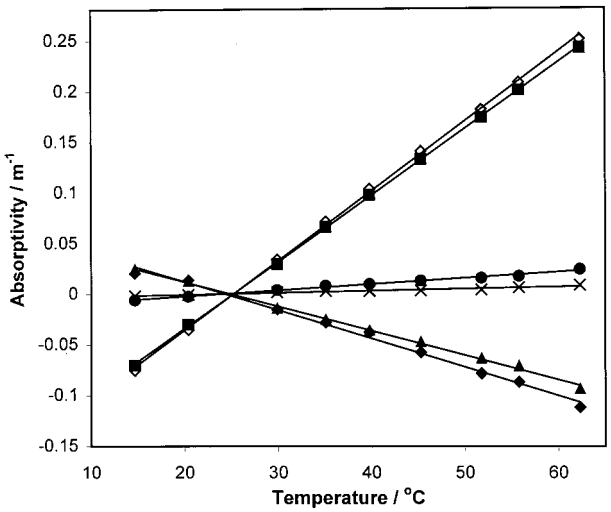

Figure 4. Linear dependences of the absorptivity upon temperature over the ~15 to 60 °C range are illustrated for the peak wavelengths of 604 (●), 660 (×), 738 (♦), 796 (▲), 836 (■), and 888 (○) nm from Figure 3.

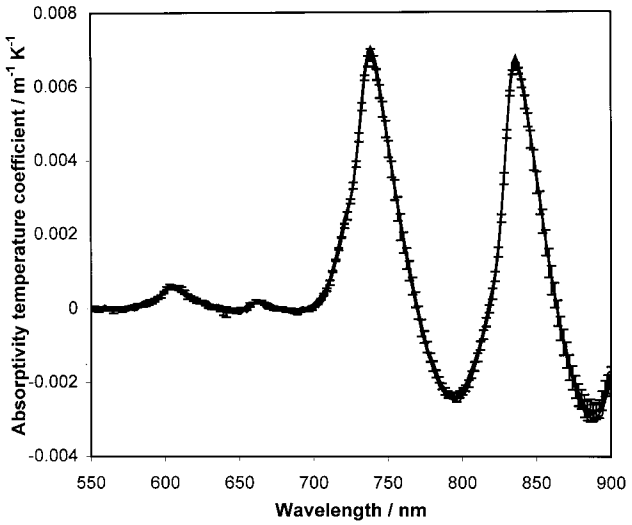

Figure 5. Absorptivity temperature coefficients (d*a*/d*T*) for the 550 to 900 nm region are shown for eight independent experiments, four of which were obtained with increasing temperature and four with decreasing temperature. For clarity, the 95% confidence interval of the absorptivity temperature coefficient is shown only for the run used as an example in Figures 2 to 4.

also compares the results of the present work with the previously published values in the 550- to 900 nm region.

Discussion

I. Comparison with Earlier Work. The literature data for the absorptivity temperature coefficient are summarized in Figure 1. The new data presented in this work are very similar to the most reliable published data of Pegau et al.[1,4,6] The data of Buiteveld et al.[5] appear subject to systematic error because their whole curve is shifted vertically, possibly due to uncorrected instrument drift as the sample temperature was increased. Because earlier workers have not purified their water, nor cleaned their glassware, as scrupulously as in the present study, we suggest that the organic impurities present in the water used by other workers have a *negligible* effect on the temperature coefficient of absorptivity in the visible and near-IR regions. Note, however, that the same is *not* true for the absolute absorptivity coefficient, which is strongly dependent on water purity.[12−15]

TABLE 1: Absorptivity Temperature Coefficients (d*a*/d*T*) as a Function of Wavelength for Liquid Water from ~15 to 60 °C and Their Associated 95% Confidence Intervals (in parentheses)

λ/nm	da/dT/(10^{-5} m^{-1} K^{-1})	λ/nm	da/dT/(10^{-5} m^{-1} K^{-1})	λ/nm	da/dT/(10^{-5} m^{-1} K^{-1})
550	4 (2)	670	7 (4)	790	−232 (4)
552	3 (3)	672	4 (3)	792	−238 (4)
554	3 (3)	674	2 (3)	794	−240 (6)
556	2 (2)	676	−1 (2)	796	−241 (6)
558	2 (3)	678	−3 (3)	798	−237 (7)
560	2 (3)	680	−5 (2)	800	−230 (5)
562	1 (3)	682	−6 (3)	802	−218 (7)
564	0 (3)	684	−6 (3)	804	−203 (8)
566	−1 (2)	686	−7 (2)	806	−183 (7)
568	1 (3)	688	−7 (3)	808	−160 (6)
570	0 (3)	690	−5 (4)	810	−133 (6)
572	0 (4)	692	−3 (4)	812	−104 (5)
574	1 (4)	694	−2 (3)	814	−73 (6)
576	3 (3)	696	0 (2)	816	−41 (7)
578	4 (4)	698	3 (3)	818	−4 (9)
580	6 (4)	700	8 (4)	820	33 (8)
582	9 (3)	702	13 (5)	822	80 (6)
584	12 (4)	704	21 (5)	824	148 (8)
586	16 (5)	706	31 (6)	826	238 (8)
588	18 (4)	708	45 (5)	828	341 (6)
590	20 (3)	710	64 (5)	830	465 (7)
592	22 (3)	712	89 (5)	832	577 (8)
594	26 (3)	714	118 (5)	834	645 (9)
596	32 (2)	716	148 (7)	836	670 (7)
598	40 (2)	718	181 (7)	838	655 (6)
600	49 (3)	720	215 (7)	840	618 (6)
602	56 (3)	722	247 (5)	842	573 (8)
604	60 (3)	724	280 (4)	844	520 (7)
606	58 (3)	726	319 (5)	846	467 (7)
608	54 (3)	728	376 (6)	848	412 (7)
610	49 (4)	730	449 (8)	850	352 (7)
612	43 (5)	732	527 (9)	852	296 (6)
614	38 (4)	734	607 (8)	854	242 (6)
616	33 (3)	736	665 (7)	856	186 (6)
618	30 (3)	738	689 (7)	858	130 (5)
620	25 (2)	740	680 (8)	860	86 (4)
622	21 (3)	742	649 (9)	862	42 (4)
624	17 (3)	744	605 (8)	864	−6 (5)
626	15 (4)	746	553 (7)	866	−49 (5)
628	11 (5)	748	502 (6)	868	−89 (6)
630	7 (2)	750	450 (5)	870	−124 (7)
632	4 (2)	752	396 (7)	872	−156 (7)
634	1 (3)	754	341 (6)	874	−185 (4)
636	−1 (4)	756	289 (6)	876	−210 (6)
638	11 (5)	758	241 (7)	878	−234 (8)
640	−5 (4)	760	194 (6)	880	−254 (8)
642	−5 (3)	762	150 (7)	882	−269 (7)
644	−5 (3)	764	111 (6)	884	−279 (7)
646	−6 (4)	766	71 (7)	886	−282 (7)
648	−6 (4)	768	32 (6)	888	−288 (8)
650	−5 (4)	770	−4 (6)	890	−284 (12)
652	−3 (3)	772	−41 (7)	892	−280 (7)
654	0 (5)	774	−73 (6)	894	−263 (11)
656	5 (4)	776	−103 (5)	896	−236 (10)
658	11 (3)	778	−130 (5)	898	−210 (15)
660	16 (1)	780	−152 (6)	900	−183 (9)
662	18 (2)	782	−174 (6)		
664	17 (3)	784	−194 (6)		
666	13 (4)	786	−211 (5)		
668	10 (3)	788	−223 (6)		

II. Calculation of the Absolute Absorptivity at a Given Temperature. The UV−vis and near-IR absorptivity spectrum of liquid water at a single temperature has been investigated by many workers, and summarized recently by Sogandares and Fry,[13] Pope and Fry,[14] and Litjens et al.,[15] from the present group. Our present experiments were not optimized to obtain the most definitive absorption spectrum of water, but rather to

give a reliable temperature coefficient that can be used to calculate the absorptivity spectrum at any given temperature in the 15 to 60 °C temperature range from a reference spectrum at a given temperature. For this reason, we direct the reader to the single-temperature spectra of ultrapure water obtained by Pope and Fry[14] and Litjens et al.[15]

III. Temperature Dependencies of the Near-IR and Visible Absorption Spectra of Liquid Water. Weak absorption by liquid water at wavelengths longer than ~400 nm is due to excitation of higher overtone and combination transitions of water. Liquid water bands in the near-IR have moderate intensity and were assigned by Bayly et al.[16] in 1963. Patel and Tam[17,18] extended the assignments into the green region of the spectrum by using laser optoacoustic spectroscopy to resolve weak higher overtones. Observed structure in the spectrum fitted a simple anharmonic formula $\upsilon_n/\mathrm{cm}^{-1} = n \bullet (3620-63\ n)$, allowing assignment of the absorption bands at 604 and 514 nm to the fifth and sixth harmonics (fourth and fifth overtones) of the OH stretch of water. Most recently, Fry and co-workers have obtained high-quality spectra by using photothermal deflection spectroscopy[13] and an integrating cavity absorption meter.[14] Their data have enabled assignment of the sixth and seventh overtones of the water stretching vibrations at 449 and 401 nm, respectively. Because the bands are broad in liquid water, a combined assignment to the harmonics of the symmetric *and* asymmetric stretches was made. Shoulders corresponding to a combination of each harmonic with one quantum of the H_2O scissor vibration have also been identified.[14] These assignments also explain the lower absorptivity of D_2O compared with H_2O in the visible region[9,18] because the equivalent harmonics of D_2O lie at significantly longer wavelengths.

It is clear from Figure 1 that the temperature dependence of the near-IR and visible absorption spectrum of liquid water is strongest in the regions of the overtones and combination bands of the water vibrations. As the temperature rises, the intensity of each band shifts from the lower side of the absorption envelope to the higher energy side. The temperature dependence of the visible-near-IR absorption bands is very similar to that of the first overtone of the OH stretch[19−21] and to that of other combination bands at wavelengths shorter than 1.1 μm.[20]

In Figure 3, the visible and near-IR spectra of liquid water at a range of temperatures are subtracted from the spectrum obtained at 25.2 °C. Isosbestic points are observed, viz. at certain wavelengths all spectra cross at the same absorptivity. In fact, isosbestic points occur for liquid water in IR and near-IR,[19,20] visible,[4,5,7] and Raman[21,22] spectra and in X-ray diffraction data.[23−25] They arise when there are two independent components whose concentrations (and hence absorptivities) vary with temperature while their band half-widths, positions, and shapes remain invariant. In optical experiments, the isosbestic points do not persist at low[22] or high[20,21] temperatures. At high temperatures, it is probably due to the formation of a third component. At low temperatures, the water probably remains a two-component mixture, but bands shift or change shape.[25] However, the existence of distinct isosbestic points implies that liquid water at ambient pressure and below ~80 °C[20] is primarily a mixture of two spectroscopically and structurally distinct species that can be treated independently.

IV. Models of Water Structure. Early mixture models for liquid water, such as those based around IR, near-IR, and Raman data, often described the components in terms of the immediate hydrogen bonding of the monomer.[19,21,26] In these models, a water molecule was described as being fully hydrogen bonded if it had four hydrogen bonds: two via its lone pairs and two via its hydrogen atoms. Hence these molecules were said to have "ice-like" bonding. In contrast, partially hydrogen-bonded water molecules had one or more broken hydrogen bonds. Despite the apparent success of such models in describing the IR, near-IR, visible and Raman spectra, they do not satisfactorily explain other properties of water.[25]

In the mid-1980s, Robinson and co-workers[27,28] developed a new two-component mixture model for the structure of liquid water that has proved extremely successful in providing a quantitative description of its properties. (See refs 25 and 29.) The model describes water as a mixture of components with ice-Ih and ice-II structures (shown in Figure 1 of ref 30), "locally rearranging on picosecond time scales with average compositions that depend on the temperature and the pressure".[25] It is a "structurally explicit two-state outer-neighbor bonding model,"[25] unlike the unsuccessful inner-neighbor models mentioned briefly above. The precise structural requirements imposed by this model are supported by the observed isosbestic points in isochoric temperature differential X-ray scattering experiments.[25,29] As the temperature of water increases, the equilibrium between the two components increasingly shifts to the ice-II structure.

This model is easily reconciled with our visible and near-IR spectra because they exhibit distinct isosbestic points characteristic of a two-component mixture.[25] At lower temperatures, the more strongly bound ice-Ih structure dominates, and we observe that the low-energy side of the overtone or combination band has higher intensity. Interestingly, McCabe et al.[19] attributed the red-most band in the first overtone region (1.45 μm) of the water absorption spectrum to an ice-like species, because its shape and position were rather like the spectra of ice-Ih. As the water temperature increases, the intensity shifts to higher energy[31] because the hydrogen-bond strength is reduced in the ice-II component,[32] thus leading to stronger OH bonds in the water molecules. From Figure 3, we notice also that as the temperature increases, the positive lobes have a greater increase in intensity than the concomitant decrease in intensity of the negative lobes. This occurs because the more strongly hydrogen-bonded molecules of the ice-Ih type have lower transition intensities in the overtone regions[26] than their more weakly bound[32] equivalents of the ice-II type.

However, there is a quantitatively stronger connection between our data and the Robinson model. Figure 4 shows the linear relationship between intensity and temperature for the peaks of the differenced absorptivity spectra, which we have used, along with the data from all wavelengths, to generate Figures 1 and 5. These results suggest that, within the Robinson model,[27,28] there is a *linear* transformation of ice-Ih structure into ice-II structure with increasing temperature. Indeed, from their fits to liquid water density data using the two-state, outer-neighbor bonding model, Robinson and co-workers[30] have obtained fractional compositions of the ice-Ih and ice-II structures as a function of temperature. Although the transformation from ice-Ih to ice-II is nonlinear over the range 0 to 100 °C, taking smaller subsets of their data (for example, 0 to 60 °C) results in close to *linear* dependence of ice-Ih structure on temperature. Thus, we find that the two-state, outer-neighbor bonding model of Robinson and co-workers provides a microscopic structural explanation for the linear temperature dependence of the absorptivity of liquid water, at least in the 0 to 60 °C region.

Conclusion

We have presented new temperature-dependent absorptivity spectra of liquid water. The data are in good agreement with

the most reliable absorptivity temperature coefficients reported previously, suggesting that the presence of organic impurities has negligible effect on the coefficients.

The linear dependence of the absorptivity of liquid water on temperature is a direct consequence of the microscopic changes in water structure that occur as the temperature increases. Specifically, the two-state, outer-neighbor bonding model of Robinson and co-workers predicts a nearly linear temperature dependence of the transformation of ice-Ih to ice-II structure, which is mirrored in the near-IR and visible spectra of the higher overtone and combination bands of H_2O.

Acknowledgment. We thank Mr Keith Stubbs for making some preliminary measurements. AJM and T.I.Q. are grateful for research support from The University of Western Australia (UWA). V.S.L. gratefully acknowledges the tenure of a special UWA postdoctoral research fellowship.

References and Notes

(1) Pegau, W. S.; Gray, D.; Zaneveld, J. R. V. *Appl. Opt.* **1997**, *36*, 6035.
(2) Bell, J. T.; Krohn, N. A. *J. Phys. Chem.* **1970**, *74*, 4006.
(3) Højerslev, N. K.; Trabjerg, I. Report 51, University of Copenhagen Inst. Phys. Oceanogr., 1990.
(4) Pegau, W. S.; Zaneveld, J. R. V. *Limnol. Oceanogr*. **1993**, *38*, 188.
(5) Buiteveld, H.; Hakvoort, J. H. M.; Donze, M. *Proc. S. P. I. E. − Int. Soc. Opt. Eng.* **1994**, *2258* (Ocean Optics XII), 174.
(6) Pegau, W. S.; Zaneveld, J. R. V. *Proc. S. P. I. E. − Int. Soc. Opt. Eng.* **1994**, *2258* (Ocean Optics XII), 597.
(7) Trabjerg, I.; Højerslev, N. K. *Appl. Opt.* **1996**, *35*, 2653.
(8) Collins, J. F. *Phys. Rev.* **1925**, *26*, 771.
(9) Waggener, W. C. *Anal. Chem.* **1958**, *30*, 1569.
(10) Luck, W. A. P. *Ber. Bunsen-Ges. Phys. Chem.* **1965**, *69*, 626.
(11) Pegau, W. S., personal communication 2001.
(12) Quickenden, T. I.; Irvin, J. A. *J. Chem. Phys.* **1980**, *72*, 4416.
(13) Sogandares, F. M.; Fry, E. S. *Appl. Opt.* **1997**, *36*, 8699.
(14) Pope, R. M.; Fry, E. S. *Appl. Opt.* **1997**, *36*, 8710.
(15) Litjens, R. A. J.; Quickenden, T. I.; Freeman, C. G. *Appl. Opt.* **1999**, *38*, 1216.
(16) Bayly, J. G.; Kartha, V. B.; Stevens, W. H. *Infrared Phys.* **1963**, *3*, 211.
(17) Patel, C. K. N.; Tam, A. C. *Nature* **1979**, *280*, 302.
(18) Tam, A. C.; Patel, C. K. N. *Appl. Opt.* **1979**, *18*, 3348.
(19) McCabe, W. C.; Subramanian, S.; Fisher, H. F. *J. Phys. Chem.* **1970**, *74*, 4360.
(20) Luck, W. A. P.; Ditter, W. *J. Phys. Chem.* **1970**, *74*, 3687.
(21) Monosmith, W. B.; Walrafen, G. E. *J. Chem. Phys.* **1984**, *81*, 669.
(22) D′Arrigo, G.; Maisano, G.; Mallamace, F.; Migliardo, P.; Wanderlingh, F. *J. Chem. Phys.* **1981**, *75*, 4264.
(23) Bosio, L.; Chen, S.-H.; Teixeira, J. *Phys. Rev. A* **1983**, *27*, 1468.
(24) Okhulkov, A. V.; Demianets, Y. N.; Gorbaty, Y. E. *J. Chem. Phys.* **1994**, *100*, 1578.
(25) Robinson, G. W.; Cho, C. H.; Urquidi, J. *J. Chem. Phys.* **1999**, *111*, 698.
(26) Symons, M. C. R. *Chem. Br.* **1989**, *25*, 491.
(27) Robinson, G. W.; Lee, J.; Bassez, M.-P. *J. Chem. Soc., Faraday Trans. 2* **1986**, *82*, 2351.
(28) Bassez, M.-P.; Lee, J.; Robinson, G. W. *J. Phys. Chem.* **1987**, *91*, 5818.
(29) Urquidi, J.; Robinson, G. W.; Cho, C. H.; Xiao, B.; Singh, S. ECCC-5 (Fifth Electronic Computational Chemistry Conference) http://www.phys.ttu.edu/∼dujcb
(30) Vedamuthu, M.; Singh, S.; Robinson, G. W. *J. Phys. Chem.* **1994**, *98*, 2222.
(31) Hobbs, P. V. *Ice Physics*; Clarendon: Oxford, UK, 1974 (pp 245−6).
(32) Jenkins, S.; Morrison, I. *Chem. Phys. Lett.* **2000**, *317*, 97.